Integrable high order UWB pulse photonic generator based on cross phase modulation in a SOA-MZI

Vanessa Moreno,[2] Manuel Rius,[1] José Mora,[1,*] Miguel A. Muriel,[2] and José Capmany[1]

[1] *ITEAM Research Institute, Universitat Politècnica de València, C/ Camino de Vera s/n, Valencia 46022, Spain*
[2]*Department of Photonics Technology and Bioengineering, ETSIT, Universidad Politécnica de Madrid (UPM), Av. Complutense 30, Madrid 28040, Spain*
[*] *jmalmer@upv.es*

Abstract: We propose and experimentally demonstrate a potentially integrable optical scheme to generate high order UWB pulses. The technique is based on exploiting the cross phase modulation generated in an InGaAsP Mach-Zehnder interferometer containing integrated semiconductor optical amplifiers, and is also adaptable to different pulse modulation formats through an optical processing unit which allows to control of the amplitude, polarity and time delay of the generated taps.

OCIS codes: (060.0060) Fiber optics and optical communications; (060.5625) Radio frequency photonics.

References and links

1. J. Yao, "Photonics for ultrawideband communications," IEEE Microw. Mag. **10**(4), 82–95 (2009).
2. J. Zheng, N. Zu, L. Wang, J. Liu, and H. Liang, "Photonic generation of ultrawideband pulse with tunable notch-band behavior," IEEE Photonics Journal **4**(3), 657–663 (2012).
3. J. Capmany and D. Novak, "Microwave photonics combines two worlds," Nat. Photonics **1**(6), 319–330 (2007).
4. F. Zeng and J. Yao, "An approach to ultrawideband pulse generation and distribution over optical fiber," IEEE Photon. Technol. Lett. **18**(7), 823–825 (2006).
5. J. Yao, F. Zeng, and Q. Wang, "Photonic generation of ultrawideband signals," J. Lightwave Technol. **25**(11), 3219–3235 (2007).
6. J. Yao, "Photonics for ultrawideband communications," IEEE Microw. Mag. **10**(4), 82–95 (2009).
7. F. Zeng and J. Yao, "All-optical bandpass microwave filter based on an electro-optic phase modulator," Opt. Express **12**(16), 3814–3819 (2004).
8. E. Zhou, X. Xu, K. Lui, and K. K.-Y. Wong, "A power-efficient ultra-wideband pulse generator based on multiple PM-IM conversions," IEEE Photon. Technol. Lett. **22**(14), 1063–1065 (2010).
9. I. Lin, J. D. McKinney, and A. M. Weiner, "Photonic synthesis of broadband microwave arbitrary waeforms applicable to ultrawideband communication," IEEE Microw. Wirel. Compon. Lett. **15**(4), 226–228 (2005).
10. A. M. Weiner, "Femtosecond pulse shaping using spatial light modulators," Rev. Sci. Instrum. **71**(5), 1929–1960 (2000).
11. J. Capmany, B. Ortega, and D. Pastor, "A tutorial on microwave photonic filters," J. Lightwave Technol. **24**(1), 201–229 (2006).
12. R. A. Minasian, "Photonic signal processing of microwave signals," IEEE Trans. Microw. Theory Tech. **54**(2), 832–846 (2006).
13. M. Bolea, J. Mora, B. Ortega, and J. Capmany, "Optical UWB pulse generator using an N tap microwave photonic filter and phase inversion adaptable to different pulse modulation formats," Opt. Express **17**(7), 5023–5032 (2009).
14. J. Dong, X. Zhang, Y. Zhang, and D. Huang, "Optical UWB doublet pulse generation using multiple nonlinearities of single SOA," Electron. Lett. **44**(18), 1083–1084 (2008).
15. F. Wang, J. Dong, E. Xu, and X. Zhang, "All-optical UWB generation and modulation using SOA-XPM effect and DWDM-based multi-channel frequency discrimination," Opt. Express **18**(24), 24588–24594 (2010).
16. B. Luo, J. Dong, and X. Zhang, "Photonic generation of UWB doublet pulse based on XPM in an SOA-based NOLM," Opto-Electronics and Communications Conference, 717–718 (2012).
17. M. D. Manzanedo, J. Mora, and J. Capmany, "Continuously tunable microwave photonic filter with negative coefficients using cross-phase modulation in an SOA-MZ interferometer," IEEE Photon. Technol. Lett. **20**(7), 526–528 (2008).

#191592 - $15.00 USD Received 4 Jun 2013; revised 5 Aug 2013; accepted 5 Aug 2013; published 23 Sep 2013

18. D. Marpaung, C. Roeloffzen, R. Heideman, A. Leinse, S. Sales, and J. Capmany, "Integrated microwave photonics," Laser & Photon. Rev. **7**(4), 506–538 (2013).
19. S. Sales, W. Xue, J. Mork, and I. Gasulla, "Slow and Fast Light Effects and their Applications to microwave photonics using Semiconductor Optical Amplifiers," IEEE Trans. Microw. Theory Tech. **58**(11), 3022–3038 (2010).
20. J. Sancho, J. Bourderionnet, J. Lloret, S. Combrié, I. Gasulla, S. Xavier, S. Sales, P. Colman, G. Lehoucq, D. Dolfi, J. Capmany, and A. De Rossi, "Integrable microwave filter based on a photonic crystal delay line," Nat Commun **3**, 1075 (2012).
21. H.-W. Chen, A. W. Fang, J. D. Peters, Z. Wang, J. Bovington, D. Liang, and J. E. Bowers, "Integrated microwave photonic filter on a hybrid silicon platform," IEEE Trans. Microw. Theory Tech. **58**(11), 3213–3219 (2010).

1. Introduction

Ultra-wide band (UWB) transmission systems are of interest in the fields of short-range communications, high-capacity wireless and broadband sensor networks [1]. The Federal Communications Commission (FCC) defined UWB technology as any wireless transmission scheme where the fractional bandwidth Δf fulfills $\Delta f / f_o \geq 20\%$ in which Δf corresponds to a −10 dB bandwidth and f_o is the center frequency of signal, or also any communications setup with more than 500 MHz of absolute bandwidth [2].

Although the FCC allows an exploitation of a very wide bandwidth region in the spectrum with a low power density to minimize interference with narrowband systems, UWB limitations have been related to its short reach and the fact that its distribution is limited to a coverage area of a few tens of meters. In this context, over the past years there has been notable interest in research oriented towards expanding the reach of UWB by developing different techniques for its generation in the optical domain [3] and its subsequent distribution over low loss optical fiber links. Indeed, it is interesting that UWB signals can be generated and distributed directly in the optical domain in order to fully exploit the advantages of photonic as light weight, small size, large tunability, reconfigurability and the immunity to electromagnetic interference [4].

UWB over fiber can be implemented with electrical passband filters available commercially by means of a conventional electrooptical conversion. In this case, the nonlinear processes present in the optical modulation and photodetection have to be considered in addition. Indeed, electronic solutions offer a specific design for transmission links with a given modulator and detector and other additional components such as an amplifier. Therefore, a filtering adaptation is needed to satisfy the FCC mask requirements which, is not found in electrical filters. In this context, direct UWB pulse generation in the optical domain can become a promising solution, and, furthermore, frequency dependence of all optical components can be taken into account together with electrical UWB pulses.

Several approaches have recently been proposed to generate UWB pulses using optical techniques [5,6]. These techniques can be classified into methods for UWB generation based on phase-modulation-to-intensity modulation conversion [7,8], optical spectral shaping and dispersion-induced frequency to-time mapping [9,10] and microwave photonic filtering [11–13]. These last approaches have demonstrated a high reconfigurability of the generated waveform due to the inherent properties of the microwave photonic filters. In this context, it is interesting to consider the design of systems where semiconductor optical amplifiers (SOAs) can be employed, in order to exploit the non-linear effects of Cross-Phase Modulation (XPM) or Cross Gain Modulation (XGM) which represent intrinsic features of these devices, commonly used for the discussed waveform generation [14–16]. Furthermore, the successful demonstration of these approaches can lead to the potential integration of the UWB generator in an optical chip.

In this paper, we propose a novel and potentially integrable scheme designed for the generation and reconfiguration of UWB pulses. The proposed experimental setup employs a set of optical sources, a pump signal generator and an amplitude electro-optical modulator (EOM). At the core of the system there are an InGaAsP SOA-Mach-Zehnder interferometer

#191592 - $15.00 USD Received 4 Jun 2013; revised 5 Aug 2013; accepted 5 Aug 2013; published 23 Sep 2013

(MZI) and an optical processing unit. Firstly, the operation principles of this structure are defined and explained. We show that the generation of a positive or a negative tap pulse is directly related to the input port selected in the interferometric structure. Secondly, we show and analyze the different variety of waveforms that can be obtained: a monocycle, a doublet and a four-coefficient pulsed UWB signal along with their corresponding spectral representations. We also demonstrate how the addition of optical sources improves the spectrum in terms of fulfilling the requirements settled by the FCC. Finally, we show that Bi-Phase Modulation (BPM) and Pulse Position Modulation (PPM) can be easily implemented using our proposed experimental layout due to the high reconfigurability of the system.

2. Principle of operation

Figure 1 shows the experimental setup proposed to generate high-order UWB pulses. It corresponds to a microwave photonic filter whose properties related to tunability and reconfigurability have been considered in [17]. The key component of this scheme is an integrated SOA-MZI. For this experimental proposal, a counter-propagation configuration was implemented. The SOA-MZI is an all optical monolithically integrated Mach-Zehnder interferometer closed by different Y-union branches. The scheme of the integrated SOA-MZI contains two 1-mm length SOAs of InGaAsP-InP. In principle, cross gain modulation (XGM) and cross phase modulation (XPM) effects can be present in this non-linear structure. However, the linewidth enhancement factor of the SOAs is large enough to neglect the effects of XGM, hence the conversion effects that we observe are a direct result of XPM.

The proposed scheme works as follows: A continuous (CW) pump signal of 13 dBm is centered at λ_{PUMP} = 1535.04 nm, connected to an electro-optical modulator (EOM) and its ouput injected into the interferometric structure through port 1. The electrical signal that feeds this EOM consists of an electrical pulse with a 12.5 Gb/s bit rate and a fixed pattern of one "1" and sixty-three "0" summing up a total of 64 bits. In Fig. 2(a), we show this pulsed electrical input signal. It features a time width of 80 ps. Also, Fig. 2(b) plots the corresponding output signal from the modulator when a biasing voltage of 3.7 V is applied. This modulated signal is introduced into the port 1 of the interferometric structure to act as the pump signal in the conversion process. Indeed, the optical pulse of Fig. 2(b), which features a time width of approximately 82 ps, is inverted in order to achieve an average optical power enough to saturate the SOA.

On the other hand, four CWs lasers were used to perform the optical conversion. The sources were centered at four different wavelengths (λ_1, λ_2, λ_3 and λ_4) at 1550.12 nm, 1550.92 nm, 1551.72 nm and 1552.52 nm, respectively. Wavelengths λ_1 and λ_2 are launched into Port 4 and wavelengths λ_3 and λ_4 into Port 5. The optical power delivered by the optical sources was set to 5 dBm for λ_1 and λ_2 and 8 dBm for λ_3 and λ_4. As previously mentioned the principle of the proposed system is based on the use of XPM in a SOA-MZI structure, which permits to obtain pulses with positive and negative polarity according to the input port to which the optical source is applied. In our approach, the phase-to-intensity conversion takes place at the output of the MZI by means of the XPM effect happening inside the SOA structure. The interference between both arms results in a phase-to-intensity conversion. Indeed, the sign of the optical tap is set by selecting the input Ports 4 or 5, the outputs of which are complementary from that corresponding to port 2.

#191592 - $15.00 USD Received 4 Jun 2013; revised 5 Aug 2013; accepted 5 Aug 2013; published 23 Sep 2013

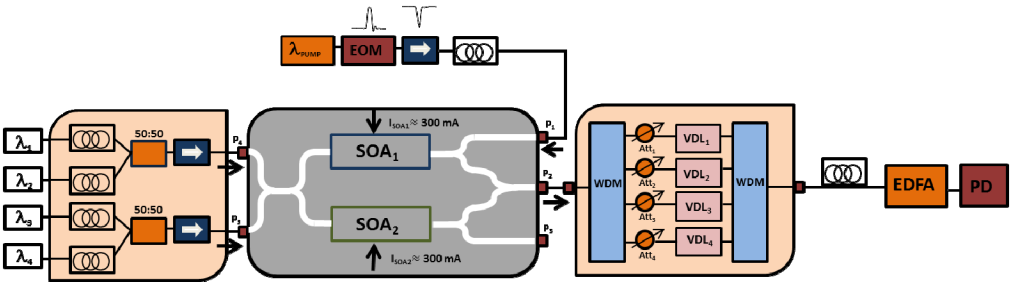

Fig. 1. Experimental layout of an optical generator for high order pulses based on a non-linear interferometric structure and an optical processor unit.

In order to test the performance of the conversion process and verify the possibility of generating pulses with opposite polarity, we first analyzed independently the positive and negative pulses generated according to the chosen input port. The process of XPM in the interferometric structure depends on the average optical power of the pump and probe signals and also it depends on the electrical currents applied to each SOA. Therefore, the optical power of the pump and probe signals have to be controlled in order to optimize the conversion process. Also, the electrical current applied to each SOA determines the XPM efficiency. In this case, SOA1 in the upper branch has a high constant current of 300 mA that determines the conversion speed of the continuous probe signal.

Figures 2(c) and 2(d) show the output signals when selecting a wavelength that generates a positive tap (λ_1 = 1550.12 nm) and a negative one (λ_3 = 1551.72 nm). Apart from the fact that the pulses show an inversion or switch in polarity, we observe that both signals have practically the same characteristics, as one should expect. The capacity for obtaining similar pulses is critical in the process of generating high order pulses. In this case, the electrical current applied to SOA2 is close to 300 mA.

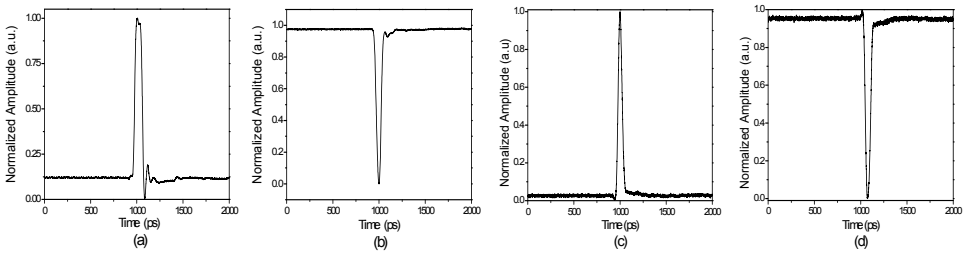

Fig. 2. Gaussian pulses of the (a) electrical signal with a 12.5 Gb/s bit rate and (b) the corresponding pump signal at the output of the EOM. Generated pulses in the system for a (c) positive pulse at λ_1 = 1550.12 nm and a (b) negative pulse at λ_3 = 1551.72 nm.

After the conversion stage, all optical modulated signals are launched into the optical processor unit to reconfigure the high order pulses by means of these optical taps. This assembly is composed by a demultiplexer (WDM) which permits to separate each optical pulse located at a different wavelength. In this way, each optical pulse is treated independently in terms of amplitude and delay by means of attenuators and variable delay lines, respectively. The WDM contains 1x40 ports but we used experimentally 4 ports. Finally, a multiplexer is employed to build the output optical pulse as a combination of the individual positive and negative optical taps which is routed to a photodetector (PD).

The proposed system could be integrated on a single chip as it is now described. Of the available technology platforms discussed in [18] for microwave photonics applications, obviously the only one leading to a monolithic approach would be that based on InP as the core of the UWB generator requires the use of a SOA based wavelength converter.

#191592 - $15.00 USD Received 4 Jun 2013; revised 5 Aug 2013; accepted 5 Aug 2013; published 23 Sep 2013

Furthermore, the array of variable attenuators could also be implemented by means of SOA devices biased below the gain transparency condition. For the implementation of delay lines one could choose between an active approach based on SOA devices as reported in [19] or by means of a more compact approach based on dispersive photonic crystal waveguide as reported in [20]. A hybrid a approach based on silicon photonics could also be employed by inserting the SOA devices in the passive silicon chip as reported in [21] for tunable MWP filters.

3. Experimental results

To demonstrate the flexible operation as an UWB generator of our proposed scheme, different signals were produced and analyzed. The main objective in each one of them was to determine the proper matching between their spectrum and the specifications of the FCC. The proposed set up comprised four laser sources, whose activation is directly related to the number of required of taps in the generated signal. The lasers were connected to the SOA-MZI which was configured through the values of currents I_{SOA1} and I_{SOA2}. As mentioned before, these currents were close to 300 mA to find an efficient conversion point [17]. The power level at the output port P2 was approximately 4dBm and the optical loss in the optical processor was close to 9 dB.

First, a monocycle was implemented by means of two laser sources, labeled as λ_1 and λ_3. The wavelength values for these probe signals were 1550.12 nm and 1550.92 nm, respectively. Each one of the employed sources was introduced through a different port which determines the polarity (λ_1 is launched into port P_4 and λ_3 into port P_5). The outcome of this setup results in a couple of similar pulses in terms of amplitude but with an inverted polarity. In terms of the equivalent microwave photonic filter, the coefficients of optical taps correspond to the pair [1,-1]. Figure 3(a) plots the time response of the monocycle pulse and Fig. 3(d) exhibits the corresponding spectrum.

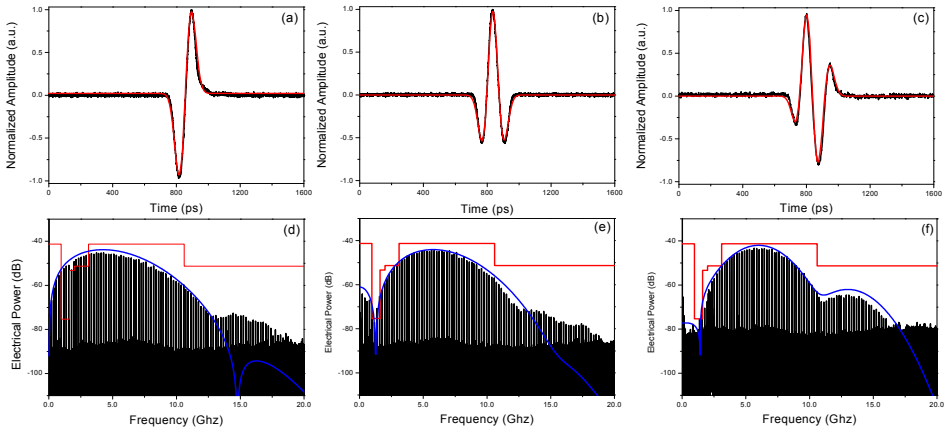

Fig. 3. Experimental (black) and theoretical(red) waveforms for (a) monocycle pulse, (b) doublet pulse and (c) high-order pulse. Corresponding spectrum (black line) for (d) monocycle, (e) doublet and (f) high-order pulses. FCC mask illustrated with a red line. Theoretical spectral representation is plotted with a blue line. The average factor is 4 for temporal traces.

In second place, a doublet was produced using three optical lasers (λ_1, λ_2 and λ_3). As in the previous case, λ_1 was launched into port P_4, λ_3 into port P_5 and the incorporated source λ_2 was introduced through port P_4. By adjusting the amplitude and delay of the introduced sources by means of the optical processing unit, it was possible to obtain a doublet with the following coefficients [-0.5, 1, −0.5]. The temporal and frequency responses of the doublet pulse are displayed in Fig. 3(b) and Fig. 3(e).

#191592 - $15.00 USD Received 4 Jun 2013; revised 5 Aug 2013; accepted 5 Aug 2013; published 23 Sep 2013

As shown in these figures, a good agreement is found between the theoretical waveforms predicted for UWB monocycles and doublets and the experimental measurements. Nevertheless, Figs. 3(d) and 3(e) do not fit properly to the FCC mask requirements despite the fact that an improvement can be observed in the obtained waveform when passing from 2 to 3 coefficients. This fact proves that the addition of suitably designed coefficients can lead to a better fit within the FCC mask.

The system is flexible enough to allow for the addition of more coefficients. For instance, by activating an additional laser source the system can generate a third-order UWB pulse. In this scenario, the previously employed inputs (λ_1, λ_2 and λ_3) were kept with the specified connections and λ_4 was introduced at port P_5. By means of the optical processing unit, we adjusted the amplitude and delay of the additional channel to obtain a combined waveform with coefficients [-0.3, 1, −1, 0.3]. For this waveform, the odd optical pulses have negative polarity while the even ones have a positive one. Figure 3(c) plots the corresponding UWB pulse and Fig. 3(f) exhibits the spectral representation, which, in this case matched the FCC mask requirements more properly than previously generated signals. In our case, the coefficients are determined quantitatively by means of a process of synthesis. Also, the system offers more flexibility than plotted since the optical processor could permit the control of 40 coefficients (1x40 WDM) but we demonstrated the system with 4 taps. In this case, the limiting factor is related to the laboratory facilities.

The previous results show that our proposed scheme features a high degree of flexibility and reconfigurability. Indeed, our approach allows for the easy implementation of different modulation formats. PPM and BPM are, for instance conventional modulation formats used in UWB communication systems, which can be implemented by different methods. In our case, BPM can be implemented by modifying the EOM bias voltage to obtain the inverted pulse or by changing the input port of the each optical tap for a given UWB pulse implementation. On the other hand, PPM can be achieved by customizing the signals amplitudes and delays according to our requirements through the optical processing unit. Figure 4 displays the measured results for generated UWB-PPM and UWB-BPM modulation signals using the monocycle, doublet and 4-tap pulse configurations.

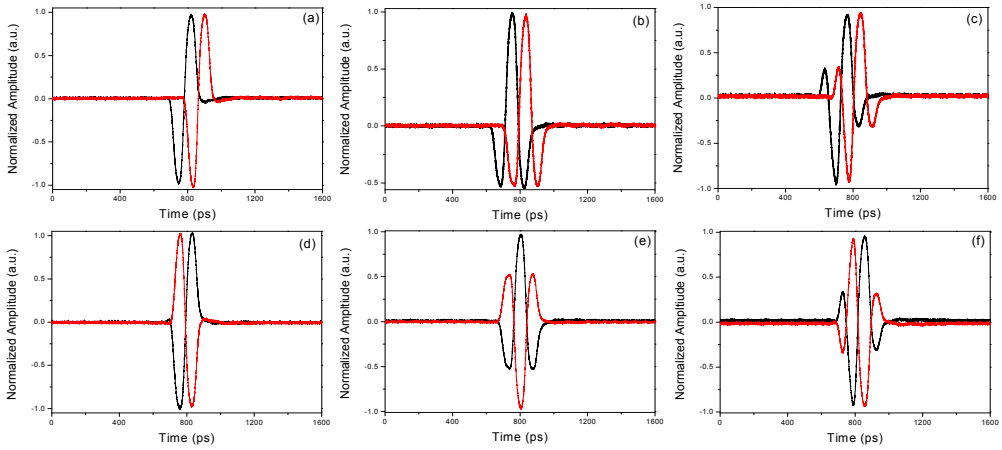

Fig. 4. PPM and BPM modulation for the generated UWB pulses. For PPM, original pulses (black line) and delayed pulses (red line) for (a) monocycle, (b) doublet and (c) four-coefficients pulse. For BPM, original pulses (black line) and inverted pulses (red line) for (d) monocycle, (e) doublet and (f) four-coefficients pulses.

In our system, the limiting factor is related to the XPM process which permits conversion up to 10 Gb/s. The electrooptical modulator and photodiode has a response of 40 Gb/s and 50

#191592 - $15.00 USD Received 4 Jun 2013; revised 5 Aug 2013; accepted 5 Aug 2013; published 23 Sep 2013

GHz, respectively. Therefore, our system is fast enough for UWB applications which feature bit rates ranging from hundreds of Mb/s to a several Gb/s.

4. Conclusions

A flexible and potentially integrable UWB pulse generation scheme for high order pulses that satisfy fully the spectrum requirements of the FCC mask has been proposed and experimentally demonstrated. The key element of the system consists of an InGaAsP SOA-MZI which leads to the generation of positive and negative pulses by exploiting XPM. The design allows an easy setup for positive and negative coefficients in terms of the equivalent microwave photonic filter. Both monocycle and doublet pulses have been successfully generated through the proposed approach, as well as a four-coefficients pulse. When compared to theoretical values, an excellent agreement between theory and experimental results can be appreciated. Finally, we have shown how the proposed scheme can de adapted to produce different modulation formats such as PPM and BPM with a single modification of the input system parameters.

Acknowledgments

The research leading to these results has been funded by the national project TEC2010-21303-C04-02 and TEC2011-26642 funded by the Ministerio de Economía y Competitividad and the projects FEDER UPVOV08-3E-008 and UPVOV10-3E-492. Miguel A. Muriel acknowledges Montse Aragon Castilla for her helpful assistance.

#191592 - $15.00 USD Received 4 Jun 2013; revised 5 Aug 2013; accepted 5 Aug 2013; published 23 Sep 2013